Proximity Effect in Gold-Coated $YBa_2Cu_3O_{7-\delta}$ Films Studied by Scanning Tunneling Spectroscopy

Amos Sharoni,[1] Itay Asulin,[1] Gad Koren,[2] and Oded Millo[1,*]

[1]*Racah Institute of Physics, The Hebrew University, Jerusalem 91904, Israel*

[2]*Department of Physics, Technion–Israel Institute of Technology, Haifa 32000, Israel*

(Received 6 July 2003; published 8 January 2004)

Scanning tunneling spectroscopy on gold layers overcoating *c*-axis $YBa_2Cu_3O_{7-\delta}$ (YBCO) films reveals proximity-induced gap structures. The gap size reduces exponentially with the distance from *a*-axis facets, indicating that the proximity effect is primarily due to the (100) YBCO facets. The penetration depth of superconductivity into the gold is ~30 nm, in good agreement with estimations for the dirty limit. The extrapolated gap at the interface is ~15 meV, similar to the value of an *s*-wave component of the order parameter measured at the YBCO surface in recent point-contact experiments.

DOI: 10.1103/PhysRevLett.92.017003 PACS numbers: 74.81.–g, 74.50.+r, 74.72.Bk

The mutual influence of a superconductor (*S*) in good electrical contact with a normal-metal (*N*), a phenomenon known as the proximity effect (PE), has been studied extensively for conventional low-temperature superconductors [1,2]. However, the picture of the PE is not as clear for the high-temperature *d*-wave superconductors, such as $YBa_2Cu_3O_{7-\delta}$ (YBCO), both experimentally and theoretically. In particular, local probe measurements of the PE, such as those performed for conventional proximity systems [3,4], are still lacking for these systems. In addition to the fundamental interest, the issue of the proximity effect is significant also from the point of view of applications, e.g., for superconductive electronic devices based on the Josephson effect.

In a homogeneous conventional (*s*-wave) superconductor, the gap in the density of states (DOS) corresponds to the superconducting pair potential (PP), a measure of the ability of quasiparticles to form Cooper pairs [5]. In an *N*-*S* proximity structure, where the PP is not spatially uniform, the gap in the DOS does not necessarily reflect the PP. Ideally, an abrupt change in the pair potential can take place at the *N*-*S* interface: from a finite PP on the *S* side, to zero on the *N* side. However, the gap in the DOS, which is a measure of the local pair amplitude, may change smoothly across the interface, from the full bulk value deep in the *S* side to zero at a distance characterized by the penetration depth into *N* [1,3,4,6,7].

For an anisotropic *d*-wave superconductor, the crystallographic orientation of the superconductor surface at the *N*-*S* interface can modify significantly the PE. For example, Josephson coupling was observed in high-temperature *S*-*N*-*S* junctions when the normal to the junction plane was along the *a* axis (transport into the *a*-*b* plane), but not when it was along the *c* axis (transport perpendicular to the *a*-*b* plane) [8,9]. This implies that Cooper pairs can leak into *N* only along the CuO_2 planes. The penetration depth (the normal coherence length), ξ_N, of the Cooper pairs into *N* was extracted from the temperature and *N*-thickness dependencies of the critical current [9–11]. However, a direct local probe measurement showing the way in which the pair amplitude decays in *N* has not yet been performed. Another unresolved issue is the symmetry of the proximity-induced order parameter in *N*, when *S* has a bulk *d*-wave PP symmetry. Theoretical calculations show that the order parameter induced in the *N* side can have an *s*-wave symmetry [12,13]. Kohen *et al.* found a $d_{x^2-y^2} + is$ PP at Au-YBCO point-contact junctions, where the *s* component showed a systematic enhancement with increased junction transparency [14], reaching a value of around 16 meV. This behavior was attributed to an unusual proximity effect that modifies the PP in YBCO near the *N*-*S* interface. In particular, it induces an *s*-wave component accompanied by a reduction in the dominant $d_{x^2-y^2}$-wave PP. A question arises now regarding the connection between this *s*-wave component and the proximity-induced order parameter at the *N* side of the interface.

The PE can be directly investigated by measuring the evolution of the proximity-induced gap in the normal-metal DOS as a function of the distance from the *N*-*S* interface, using scanning tunneling microscopy (STM) [3,4]. The magnitude of this gap is a measure of the local proximity-induced pair amplitude. In this work, we used *c*-axis YBCO films covered with gold layers of different thickness to study this gap evolution, in correlation with the gold thickness and the local surface morphology. (Unfortunately, this geometry does not allow monitoring the PE properties at the *S* side, as previously done by Levi *et al.* for Cu-NbTi junctions [3].) In the present study, the tunneling spectra revealed an exponential decay of the proximity gap with distance from *a*-axis facets. This indicates that the PE is primarily due to the interface between the normal metal and the (100) YBCO surface, and not with the (001) surface. Interestingly, while this facet selectivity reflects the in-plane versus out-of-plane anisotropy in YBCO, the tunneling spectra measured on the Au layer exhibited isotropic behavior, suggesting that the proximity-induced order parameter may have *s*-wave

symmetry. The superconductor penetration depth into the gold film was found to be $\xi_N \sim 30$ nm, in good agreement with theoretical estimations for the dirty limit, and the extrapolated gap at the interface was about 15 meV, in accordance with the above observation of Kohen *et al.* [14].

Optimally doped epitaxial YBCO films of 50 nm thickness were grown on (100) $SrTiO_3$ wafers by laser ablation deposition, with *c*-axis orientation normal to the substrate (confirmed using x-ray diffraction), as described elsewhere [15]. Next, a gold layer was deposited *in situ* by laser ablation at a temperature of 150 °C at a rate of 1 Å/s and annealed for 1 h at this temperature before cooling down to room temperature. A total of 12 samples were prepared with gold thickness varying between 1.5 and 60 nm. A bare reference YBCO film showed a sharp (0.5 K wide) transition at 90 K and gap values of 18 to 20 meV. The samples were transferred from the growth chamber in a dry atmosphere and introduced into our cryogenic STM after being exposed to ambient air for less than 15 min. The YBCO films consisted of nearly square-shaped *c*-axis crystallites, 50–100 nm lateral size and 10–15 nm height [15,16], which had relatively large (100) facets. The tunneling spectra measured on top of the bare YBCO crystallites exhibited (by and large) *V*-shaped gap structures typical of *c*-axis tunneling [15], further confirming the assigned crystallographic orientation. This crystalline structure was clearly observed, yet somewhat smeared, even after deposition of the thickest Au layer. The gold films revealed a granular morphology with surface grains of ~10 nm in lateral size and rms height roughness of up to 1.5 nm (see Fig. 1).

Tunneling spectra (dI/dV vs V characteristics) were obtained by numerical differentiation of *I*-*V* curves that were measured in correlation with the topography by momentarily disconnecting the feedback loop. About ten curves were acquired at each position to assure data reproducibility. We also checked the dependence of the tunneling spectra on the voltage and current settings (i.e., the tip-sample distance, or the tunneling resistance values—in the range of 100 MΩ to 1 GΩ) and found no effect on the measured gap features. This rules out the possibility that these gaps are even partially related to single electron charging effects [17].

A correlated topography/spectroscopy measurement manifesting the evolution of the gap structure with the distance from the crystallite *a*-axis facet is presented in Fig. 2. The topographic image in Fig. 2(a) is of a 30 nm thick Au layer coating a YBCO film, showing a crystallite of about 90 nm in size (two edges are marked by white dashed lines). Tunneling spectra were obtained sequentially along the line marked by the arrow and are presented in Fig. 2(b). The energy gap values were determined from the positions at which sharp changes of the slope were observed in the tunneling spectra (as marked by the arrow for the spectrum of the 2 meV gap). It is

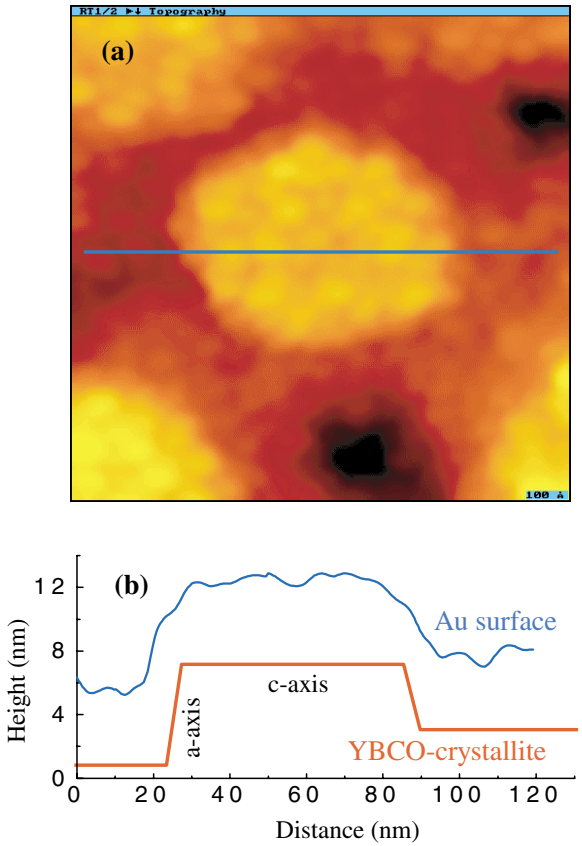

FIG. 1 (color online). (a) Topographic STM image (100×100 nm^2) of a YBCO film coated by a 5 nm thick Au layer, showing a YBCO crystallite with clear facets and the granular morphology of the Au film. (b) A cross section measured along the line drawn in (a) is shown together with a schematic cross section of the underlying YBCO crystallite, with labeled facets.

evident that the gap size reduces with increased distance from the crystallite edge, and at the same time the zero bias conductance increases. As discussed in details in Ref. [15], such edges typically expose the (100) YBCO surface. Note that the maximal observed gap just at the edge, $\Delta = 6.7$ meV, is still much smaller than the 20 meV gap of the bare YBCO sample. This is consistent with the presence of the Au layer that determines a minimal distance from the *N*-*S* interface, corresponding to the Au film thickness [see Fig. 1(b)]. At larger distances from the edge, even for thinner gold layers, the gap structure practically vanished (due to the increase of the zero bias conductance it was hard to detect gap values much smaller than 2 meV).

The results described above clearly indicate that the PE originates primarily at the *a*-axis YBCO surface, whereas the contribution of the *c*-axis surface is negligible, in agreement with previous studies of the Josephson effect in related systems [8]. This behavior reflects the quasi-two-dimensional *d*-wave symmetry of the order parameter in YBCO. However, no clear indication of *d*-wave symmetry was found for the proximity-induced pair

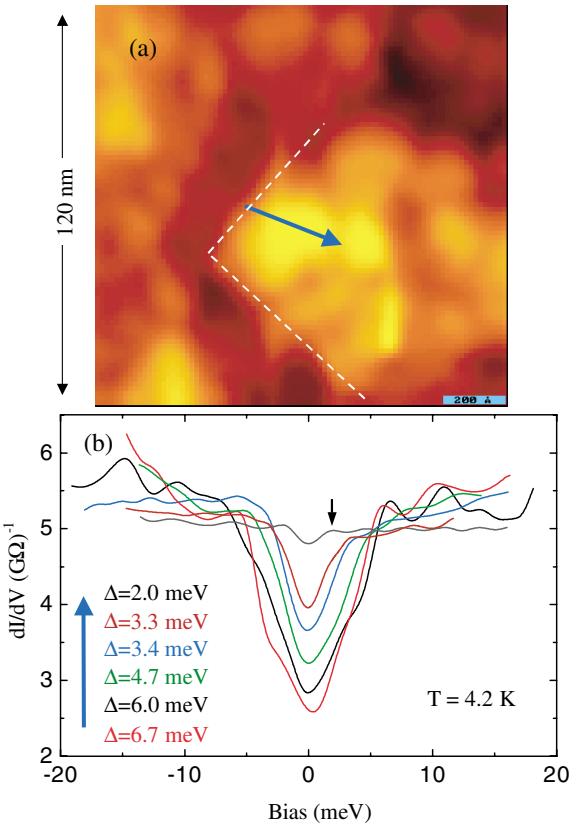

FIG. 2 (color online). A typical measurement showing the decrease in gap size as a function of the distance from a (100) facet at a crystallite edge. (a) Topographic image showing a YBCO crystallite coated with 30 nm Au. The white dashed lines mark the YBCO crystallite edges, exposing (100) facets. (b) Tunneling spectra measured along the arrow shown in (a). The gap sizes are denoted, from 6.7 meV (near the crystal edge) to 2 meV (the smallest detectable gap, with gap edge marked by the arrow). Note the corresponding increase of the zero bias conductance.

amplitude in gold. Unlike our previous observations for YBCO films [15], the measured tunneling spectra did not exhibit anisotropy when measured on different faces of a gold grain. In particular, zero bias conductance peaks (ZBCP), which appear in tunneling spectra measured on the (110) surface of pure YBCO and were observed also on (110) nanofacets in c- and a-axis films [14,18], have never been observed on gold proximity layers thicker than 7 nm (on the verge of full gold coverage). They were observed only rarely for the thinnest layers that we measured, 5 nm thick and less. It should be pointed out, however, that (110) facets in the underlying YBCO films were not abundant in our samples (as revealed in our measurements of the bare YBCO film). We therefore measured (110) YBCO films overcoated by Au layers of various thickness. This latter study (to be published elsewhere) shows that the ZBCP decays significantly faster as compared to the present proximity-induced gap and was hardly observed on Au films thicker than 16 nm (smaller than ξ_N; see below). The proximity-induced order parameter thus appears to lack clear d-wave signature and may possibly be predominantly s wave in nature, as is further discussed below.

In Fig. 3 we display an accumulation of the proximity gaps measured on the gold surface as a function of the distance to the closest (relevant) S-N interface (solid circles). This distance was determined from the distance to the crystallite edge, measured from the STM topographic images, taking into account the nominal thickness of the gold film (that in many cases was larger than the lateral distance to the crystallite edge). The solid line represents a best fit to the standard exponential decay form of the gap [1,6], $\Delta(x) = \Delta_0 \exp(-x/\xi_N)$. This fit was obtained for a penetration depth (normal coherence length) of $\xi_N \approx 29$ nm, and an interface gap value $\Delta_0 \approx 15$ meV. Note that the value of ξ_N is much larger than the rms roughness of the gold films (less than 1.5 nm); thus local height fluctuations of the Au layer do not affect much the measured gaps.

The value extracted for the penetration depth is very close to that estimated for the dirty limit [1], $\xi_N = (\frac{\hbar V_{FN} l_N}{6\pi k_B T}) \approx 33$ nm. The latter estimation was obtained assuming that the elastic mean free path l_N in the gold film is governed by grain boundary scattering, thus $l_N \sim 10$ nm, and taking the Fermi velocity in gold from the literature, $V_{FN} = 1.4 \times 10^6$ m/s.

More interesting is the value we found for Δ_0. This value is similar to the magnitude of the s-wave order parameter component observed in YBCO in the point-contact experiments of Kohen *et al.* [14], for the most

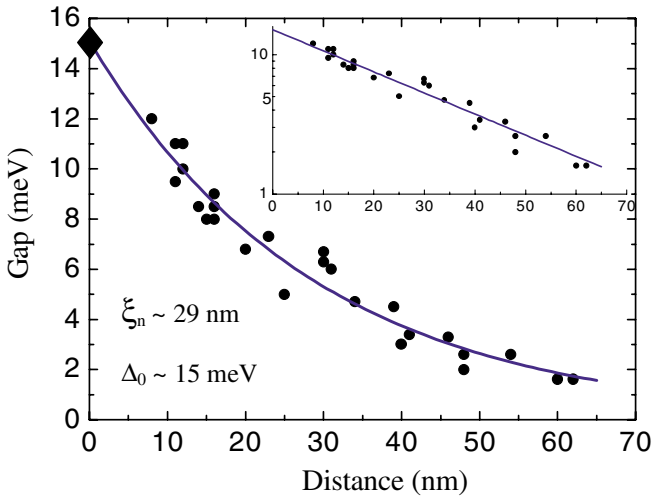

FIG. 3 (color online). Measured gap size as a function of distance from the N-S interface (solid circles). The distance is estimated from the distance to the crystallite edge, measured form the STM topographic images, taking into account the nominal Au film thickness. The solid line is a fit to a decaying exponential form, with normal coherence length (penetration depth) $\xi_N \approx 29$ nm, and interface gap value $\Delta_0 \approx 15$ meV (the diamond symbol). The inset shows the data in a semilog scale.

transparent Au-YBCO junctions measured. This *s*-wave component induced near the surface of YBCO, which has a dominant $d_{x^2-y^2}$-wave order parameter, was attributed to an anomalous *N*-*S* proximity effect. We expect that in our samples the Au-YBCO electrical contact (or junction transparency) is at least as good as in the most transparent junctions reported in Ref. [14], since our Au films were deposited onto the YBCO surface *in situ*, without breaking the vacuum. Therefore, a strong *s*-wave component may be induced at the YBCO-Au interface also in our case. It is possible then that this component plays a significant role in inducing the (isotropic) pair amplitude at the *N* side of the Au-YBCO junctions.

In summary, tunneling spectroscopy correlated with topographic measurements was used to observe the proximity effect on the normal side of highly transparent YBCO-Au junctions. The proximity-induced gap in Au decays exponentially with distance from *a*-axis YBCO facets, indicating that the PE is primarily due to the (100) YBCO surface. While this facet selectivity reflects the anisotropic nature of superconductivity in YBCO, the proximity-induced order parameter appeared to be isotropic, possibly of dominant *s*-wave symmetry. Interestingly, the interface gap correlates well with the recently observed proximity-induced *s*-wave order parameter in YBCO [14], and the coherence length in Au, $\xi_N \sim 30$ nm, conforms to "conventional" PE in the dirty limit.

We are grateful to Guy Deutscher for stimulating discussions that led to the conclusion that the most relevant length scale in our experiment is the distance from an *a*-axis facet and not the Au thickness. We also thank Amir Kohen for helpful discussions. The research was supported in part by the Israel Science Foundation and by the Heinrich Hertz Minerva center for high-temperature superconductivity.

*Electronic address: milode@vms.huji.ac.il

[1] G. Deutscher and P. G. de Gennes, *Superconductivity* (Marcel Dekker, Inc., New York, 1969).
[2] E. L. Wolf, *Principles of Electron Tunneling Spectroscopy* (Oxford University Press, New York, 1985).
[3] Y. Levi, O. Millo, N. D. Rizzo, D. E. Prober, and L. R. Motowidlo, Phys. Rev. B **58**, 15 128 (1998).
[4] N. Moussy, H. Courtois, and B. Pannetier, Europhys. Lett. **55**, 861 (2001).
[5] P. G. de Gennes, *Superconductivity of Metals and Alloys* (Benjamin, New York, 1966).
[6] W. Belzig, C. Bruder, and G. Schon, Phys. Rev. B **54**, 9443 (1996).
[7] S. Gueron, H. Pothier, N. O. Birge, D. Esteve, and M. H. Devoret, Phys. Rev. Lett. **77**, 3025 (1996).
[8] M. A. M. Gijs, D. Scholten, Th. van Rooy, and A. M. Gerrits, Appl. Phys. Lett. **57**, 2600 (1990).
[9] H. Z. Durusoy, D. Lew, L. Lombardo, A. Kapitulnik, T. H. Geballe, and M. R. Beasley, Physica (Amsterdam) **266C**, 253 (1996).
[10] E. Polturak, G. Koren, D. Cohen, E. Aharoni, and G. Deutscher, Phys. Rev. Lett. **67**, 3038 (1991).
[11] J. Gao, W. A. M. Aarnink, G. J. Gerritsma, and H. Rogalla, Physica (Amsterdam) **171C**, 126 (1990).
[12] Y. Ohashi, J. Phys. Soc. Jpn. **65**, 823 (1996).
[13] A. A. Golubov and M. Y. Kpriyanov, JETP Lett. **67**, 501 (1998).
[14] A. Kohen, G. Leibovitch, and G. Deutscher, Phys. Rev. Lett. **90**, 207005 (2003).
[15] A. Sharoni, G. Koren, and O. Millo, Europhys. Lett. **54**, 675 (2001).
[16] O. Nesher, G. Koren, E. Polturak, and G. Deutscher, Appl. Phys. Lett. **72**, 1769 (1996).
[17] E. Bar-Sadeh and O. Millo, Phys. Rev. B **53**, 3482 (1996).
[18] A. Sharoni, G. Leibovitch, A. Kohen, R. Beck, G. Deutscher, G. Koren, and O. Millo, Europhys. Lett. **62**, 883 (2003).